Available online at www.sciencedirect.com
ScienceDirect
Journal of Power Sources 161 (2006) 541–544
JOURNAL OF POWER SOURCES
www.elsevier.com/locate/jpowsour

Electrochemical properties of NiO–Ni nanocomposite as anode material for lithium ion batteries

X.H. Huang, J.P. Tu*, B. Zhang, C.Q. Zhang, Y. Li, Y.F. Yuan, H.M. Wu

Department of Materials Science and Engineering, Zhejiang University, Hangzhou 310027, China

Received 21 January 2006; received in revised form 14 March 2006; accepted 16 March 2006
Available online 11 May 2006

Abstract

NiO–Ni nanocomposite was prepared by calcining a mixture of $Ni_2(OH)_2CO_3$ and ethanol in a tube furnace at 700 °C for 45 min in air. The microstructure and morphology of the powders were characterized by means of X-ray diffraction (XRD) and transmission electron microscopy (TEM). In the composite, nanoscale Ni particles (<10 nm) were dispersed in the NiO matrix (about 100 nm). Electrochemical tests showed that the nanocomposite had higher initial and reversible capacity than pure NiO. The presence of the nanoscale Ni phase had improved both of the initial coulombic efficiency and the cycling performance, due to its catalytic activity, which would facilitate the decomposition of Li_2O and the SEI during the charge process.

Keywords: NiO; Nanoscale Ni; Composite; Anode material; Lithium ion battery

1. Introduction

During the past decade, the research on anode materials for lithium ion batteries mainly focused on searching for carbon alternatives with larger capacities and better cycling performances [1]. These materials were: (i) alloys with an active component and inactive components toward Li which acted as buffering matrix, (ii) amorphous tin-based oxides (ATCO) proposed by Fuji Co [2], and (iii) layer structured materials such as $Li_{3-x}Co_xN$ and $Li_{3-x}Ni_xN$. Recently, Tarascon and co-workers reported that transition-metal oxides (MO, where M is Fe, Co, Ni, Cu or Mn which were inactive towards Li) could be a new class of anode materials for lithium ion batteries. These transition-metal oxides demonstrated electrochemical capacities of about 700 mAh g^{-1} and excellent cycling performances [3]. These oxides with rock-salt structure have no sites for insertion/deinsertion of Li ions. There is a new mechanism which can be written as: $M_xO_y + 2yLi \leftrightarrow yLi_2O + xM$. During the discharge, the M_xO_y particle is completely disintegrated into highly dispersed metallic nanoparticles (<10 nm) and Li_2O matrix, but the global shape of the starting particle is preserved. During the subsequent charge, the Li_2O matrix decomposes and M nanoparticles convert back to M_xO_y nanograins. The occurring of this thermodynamically infeasible reaction is attributed to the highly active metallic nanoparticles [1]. Solid electrolyte interface (SEI) will also be formed during the discharge process, but it can be partially decomposed during the subsequent charge process, which is attributed to the catalytic activity of metallic nanoparticles [4]. The partially reversible formation/decomposition of SEI will lead to an extra capacity.

NiO has a theoretic capacity of 718 mAh g^{-1} when it is used as anode material for lithium ion batteries. The cycling performance of NiO is worse than that of other transition metal oxides such as CoO, CuO, and Cu_2O, but it has a higher reversible capacity than CuO and Cu_2O [3,5], and it is less expensive than CoO. Since the mechanism involves the reduction and oxidation of the active Ni nanoparticles, an increase in the content of the nanoscale Ni has the possibility to facilitate the decomposition of Li_2O and the SEI film during the charge process. In this present work, NiO–Ni nanocomposite was synthesized by a simple method, and the electrochemical properties of the nanocomposite as anode material for lithium-ion batteries were investigated.

* Corresponding author. Tel.: +86 571 87952573; fax: +86 571 87952856.
E-mail address: tujp@cmsce.zju.edu.cn (J.P. Tu).

0378-7753/$ – see front matter © 2006 Elsevier B.V. All rights reserved.
doi:10.1016/j.jpowsour.2006.03.039

2. Experimental

$Ni_2(OH)_2CO_3$ precursor was prepared as follows. $Ni(NO_3)_2 \cdot 6H_2O$ was dissolved in a ethanol–water (1:4 v/v) solvent and a green solution was formed. NH_4HCO_3 solution was added by drop under magnetic stirring until the pH value reached 7.5 upon which a light green precipitate formed. The precipitation was centrifugalized and washed with distilled water first, and then with ethanol, for three times respectively. Afterwards, the precipitation was calcined in air in a quartz tube furnace, which had been already heated to 700 °C, and was then taken out immediately (quenched in air) after 45 min. For comparison, the precipitation dried at 100 °C for 12 h in vacuum was calcined in a furnace at 700 °C under flowing oxygen for 45 min and cooled down with the furnace.

The structure and morphology of these products were characterized by X-ray diffraction (XRD, Rigaku D/max-rA; Cu Kα radiation) and transmission electron microscope (TEM, JEOL, JEM200CX). The content of each element in the materials was analyzed by energy dispersive X-ray spectrometry (EDS).

The working electrodes were prepared by a slurry coating procedure. The slurry consisted of 70 wt.% active materials, 15 wt.% acetylene black and 15 wt.% polyvinylidene fluoride (PVDF) dissolved in *N*-methyl pyrrolidinone (NMP), and was coated on a copper foam of 1.3 cm in diameter acted as current collector. The foam was pressed under a pressure of 20 MPa after drying at 120 °C for 12 h in vacuum. Test cells were assembled in an argon-filled glove box using Li foil as counter electrode, polypropylene (PP) film (Celgard 2300) as separator. The electrolyte was 1 M $LiPF_6$ in a 50:50 (w/w) mixture of ethylene carbonate (EC) and diethyl carbonate (DEC).

The galvanostatic charge–discharge tests were conducted on a PCPT-138-32D battery program-control test system with the cut-off voltages of 0.02 and 3.0 V (versus Li/Li^+) under a specific current density of 100 mA g^{-1}. Cyclic voltammetric (CV) measurements of the electrodes were performed on a CHI604B Electrochemical Workstation with a scan rate of 0.1 mV s^{-1} between 0 and 3 V (versus Li/Li^+).

3. Results and discussion

3.1. Characterization of materials

The XRD patterns of the as-synthesized powders are given in Fig. 1. Pattern (a) shows Bragg reflections of NiO and Ni phase.

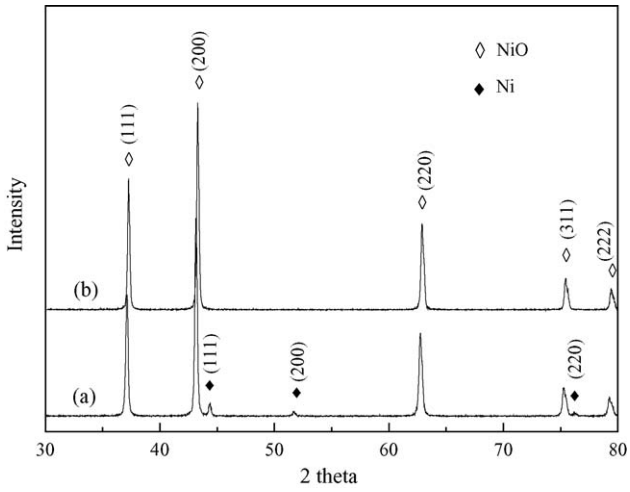

Fig. 1. XRD patterns of as-synthesized powders: (a) prepared in air and (b) prepared in oxygen.

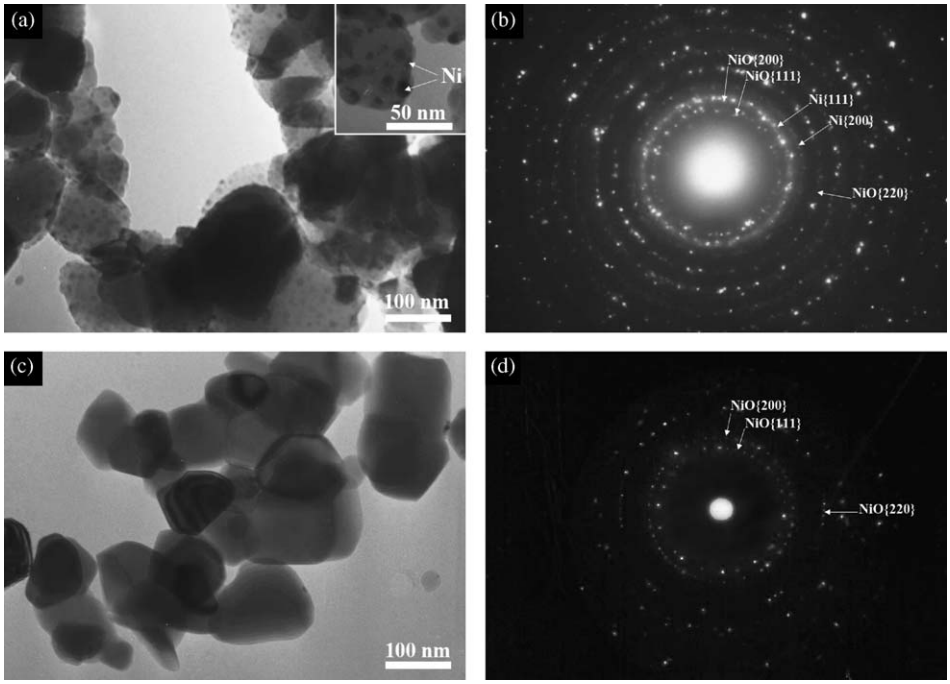

Fig. 2. (a) TEM image of the NiO–Ni composite, in the top right being a magnification image. (b) SAED pattern for the NiO–Ni composite. (c) TEM image of the NiO. (d) SAED pattern for the NiO.

This indicates that the sample prepared in air is composite of NiO and Ni. The weak Ni peaks indicate a low quantity of Ni. In pattern (b), all peaks can be index to a single NiO phase. This indicates that the sample prepared in oxygen is pure NiO.

EDS results show that the content of element Ni and O for the NiO sample are 47.84 and 52.16 at.%, respectively. The content of O is higher than that of Ni, as NiO is a p-type semiconductor, which has vacancies of Ni^{2+} in the lattice and can be written as: $Ni_{1-y}O$. However, in the NiO–Ni composite, the content of Ni (56.64%) is higher than that of O (43.36%). This indicates that the composite consists of NiO and Ni, which is in agreement with the XRD result.

Fig. 2 shows the TEM images and SAED patterns of the two samples. It is observed clearly that the global particles of the NiO–Ni composite are about 100 nm in sizes, as shown in Fig. 2a. In the magnification image (top right), small particles (less than 10 nm) are distributed on the global particle. According to the SAED pattern (Fig. 2b), it can be concluded that these small particles are Ni phase. Well-crystallized particles with about 100 nm in sizes can be seen in the TEM image (Fig. 2c) for the pure NiO sample, and no other phases can be observed both in the TEM image and the SAED pattern (Fig. 2d). These results are in agreement with the XRD patterns.

3.2. Electrochemical analysis

Fig. 3 shows the first galvanostatic discharge–charge and the second discharge curves for the two samples measured between 0.02 and 3.0 V versus Li/Li^+ at a current density of 100 mA g^{-1}. There is an abrupt drop in potential down to about 0.6 V in the first discharge curve for each sample, followed by a long plateau between 0.5 and 0.6 V. Both samples exhibit capacities much higher than theoretical value for NiO → Ni reduction. The extra capacity could be attributed to the formation of the SEI coating on the particles during the discharge process [6]. However, the first charge process exhibits a higher voltage with two sloping potential ranges at about 1.5 and 2.25 V, respectively, and less capacity than that of the first discharge. The irreversible capacity loss between the first discharge and charge is attributed to the incomplete decomposition of both of the SEI and Li_2O. In the second discharge, the plateau appears at about 1.25 V, which is higher than that of the first discharge.

The first discharge capacity for the NiO–Ni composite (1152.4 mAh g^{-1}) is higher than that of the NiO electrode (997.4 mAh g^{-1}). It may be attributed to the large quantity of lattice defects in the NiO–Ni composite, which was quenched from 700 °C to room temperature in air. Most defects caused by the high temperature were preserved during the quenching. These defects may provide sites for the insertion of Li ions. The initial coulombic efficiency for the NiO material is 64.9%, which is consistent with Tarascon and co-workers' results (about 65%) [3,5]. However, the NiO–Ni composite gets a higher initial coulombic efficiency (71.2%). As discussed before, highly dispersed Ni nanoparticles in the composite have catalytic activity. For the pure NiO, the Ni nanoparticles can be only result from the decomposition of the starting NiO during the discharge. As these Ni nanoparticles will convert back to NiO during the charge process, the decomposition of the SEI will be incompletely because of the lack of the catalytic Ni nanoparticles. However, for the NiO–Ni composite, as the NiO particles are dotted with nanoscale Ni particles, some active Ni will be present in the form of simple substance during the whole discharge-charge cycle. More SEI will decompose in this Ni-rich material compared to the pure NiO. At the same time, the decomposition of Li_2O will be more completely since there is enough active Ni for the reverse reaction (charge process). This is the reason for the higher coulombic efficiency. Similar results were obtained by the ball-milled Ni–Co_3O_4 composite prepared by Kang et al. [7,8].

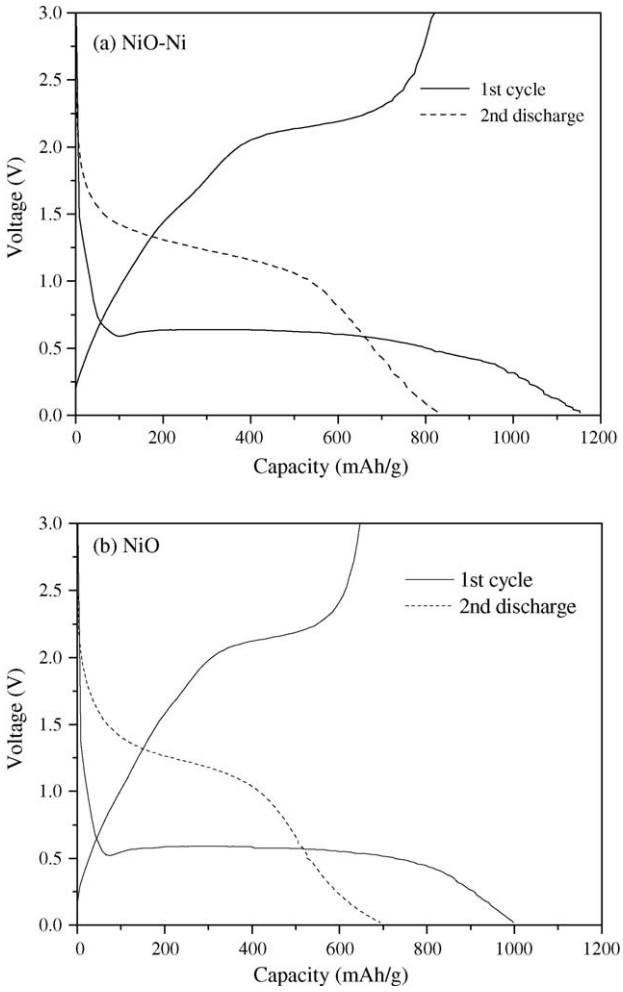

Fig. 3. Curves of the first cycles and the second discharge for: (a) NiO–Ni nanocomposite and (b) NiO.

The cyclic voltammetric curves of the NiO–Ni nanocomposite and NiO between 0 and 3 V (versus Li/Li^+) are shown in Fig. 4. Both samples exhibit similar curves. It can be seen that there are significant differences between the first scan and the subsequent scans. There is a strong peak at 0.25–0.5 V in the first cathodic scan, corresponding to the decomposition of NiO into Ni, and the formation of amorphous Li_2O and the SEI. This peak becomes broader and weaker, and shifts to about 1.2 V at the subsequent scans. There are two board peaks located at about 1.5

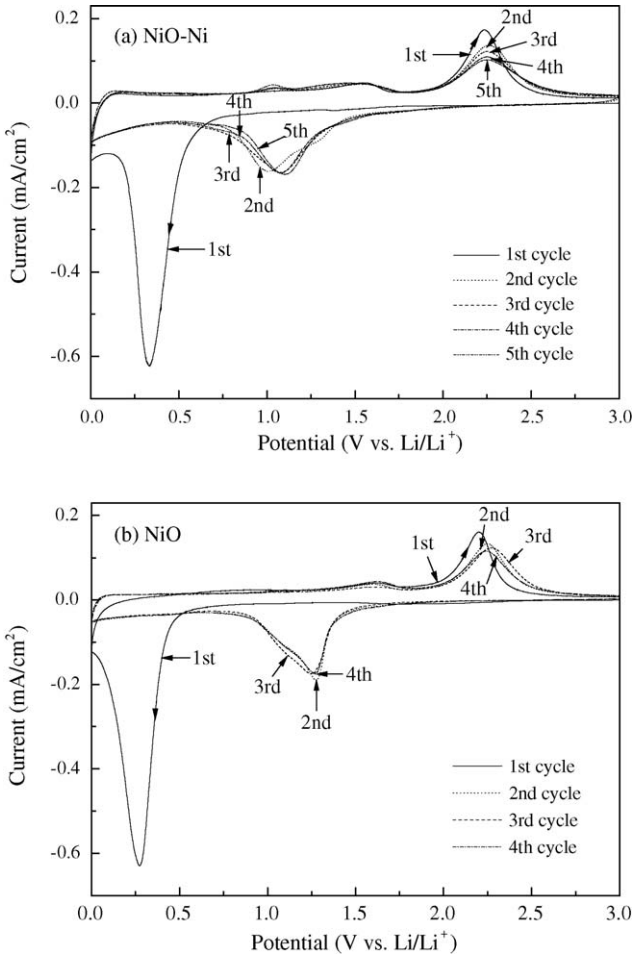

Fig. 4. Cyclic voltammograms for: (a) NiO–Ni nanocomposite and (b) NiO.

and 2.25 V in the anodic scan curves, which could be attributed to the decomposition of the SEI and Li_2O, respectively [4,6]. There is a little peak shift during the subsequent scans. The peaks in the cyclic voltammetric curves are consistent with the plateaus or sloping potential ranges in the voltage–capacity profiles. A little stronger polarization is observed in the voltammograms for the NiO–Ni electrode, which may be attributed to the defects in the crystal, since the lithium intercalated in the defects may be more difficult to deintercalate during the charge.

Fig. 5 shows the capacity retention properties of the NiO–Ni nanocomposite and NiO electrodes. The NiO–Ni nanocomposite exhibits much higher reversible capacities and much better cycling performance than the NiO. At the early stage (before the 25th cycle) of cycling, the reversible capacities for the NiO–Ni nanocomposite are higher than the theoretic value. These results can be attributed to the nanoscale Ni particles in the composite, as discussed above. For the NiO–Ni composite, the more complete decomposition of the Li_2O and SEI with poor electronic conductivity will improve the conductance of the material and the Ni phase itself may improve the electric conductivity. Other possible reason is that quantities of defects in the NiO–Ni nanocomposite will not only provide sites for the insertion of Li ions, but also will facilitate the diffusion of the ions.

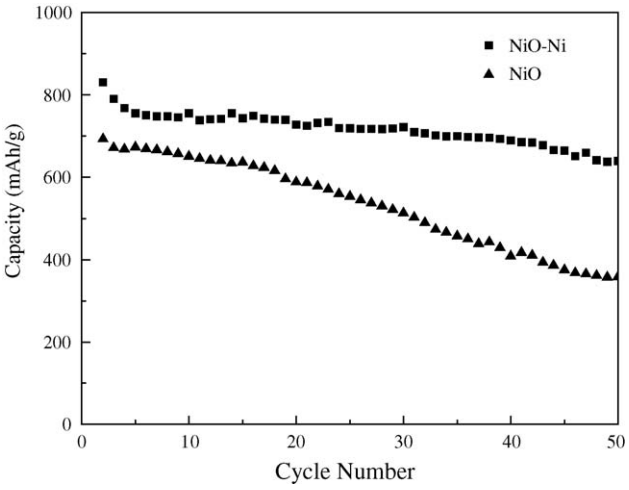

Fig. 5. Cycling performances for the NiO–Ni nanocomposite and NiO (2–50th cycle).

4. Conclusions

NiO–Ni nanocomposite material was synthesized successfully. This material has higher initial and reversible discharge capacity, higher initial coulombic efficiency, and much better cycling performance than the pure NiO. And at the early stage of cycling, the reversible capacities of the NiO–Ni nanocomposite are higher than the theoretic value of NiO. The improvement of these properties can be attributed to the presence of nanoscale Ni particles in the composite, and quantities of defects preserved by the quenching.

References

[1] J.-M. Tarascon, M. Armand, Nature 414 (2001) 359.
[2] Y. Idota, T. Kubota, A. Matsufuji, Y. Maekawa, T. Miyasaka, Science 276 (1997) 1395.
[3] P. Poizot, S. Laruelle, S. Dupont, J.-M. Tarascon, Nature 407 (2000) 496.
[4] S. Grugeon, S. Laruelle, R. Herrera-Urbina, L. Dupont, P. Poizot, J.-M. Trarscon, J. Electrochem. Soc. 148 (2001) A285.
[5] P. Poizot, S. Laruelle, S. Grugeon, J.-M. Tarascon, J. Electrochem. Soc. 149 (2002) A1212.
[6] A. Débart, L. Dupont, P. Poizot, J.-B. Leriche, J.M. Tarascon, J. Electrochem. Soc. 148 (2001) A1266.
[7] Y.M. Kang, K.T. Kim, K.Y. Lee, S.J. Lee, J.H. Jung, J.Y. Lee, J. Electrochem. Soc. 150 (2003) A1538.
[8] Y.M. Kang, K.T. Kim, J.H. Kim, H.S. Kim, P.S. Lee, J.Y. Lee, H.K. Liu, S.X. Dou, J. Power Sources 133 (2004) 252.